Case Study

Houfeng Bridge Failure in Taiwan

Jian-Hao Hong[1]; Yee-Meng Chiew, M.ASCE[2]; Jau-Yau Lu, M.ASCE[3]; Jihn-Sung Lai[4]; and Yung-Bin Lin[5]

Abstract: Failures of bridges that span a waterway often result from scour and channel instability near the bridge foundations. The Houfeng Bridge, which crosses the Da-Chia River in central Taiwan, collapsed in the 2008 typhoon flood event. On the basis of the historical records and survey of related data just after the collapse of the bridge, a methodology for the assessment of scour depth, including long-term general scour caused by earthquake and impinging jet scour generated by a concrete encased pipeline, is illustrated in the present study. The proposed method provides reasonable estimates for various scour components, which implies that before constructing a new or rebuilding an old bridge, one should use proper methodology and formulas to evaluate the scour potential and improve the bridge design, especially for bridges that are founded around the Houfeng Bridge. This case study also highlights the important effect of long-term general scour on bridge stability. In addition, a lesson is learned from this case study regarding the importance of bridge operation. **DOI: 10.1061/(ASCE)HY.1943-7900.0000430.**

CE Database subject headings: Bridge failures; Scour; Piers; Unsteady flow; Taiwan.

Author keywords: Bridge failure; Scour; Bridge pier; Unsteady flow.

Introduction

Taiwan is one of the archipelagos of islands in East Asia that frequently are exposed to two different major natural hazards: typhoons and earthquakes. Many rivers in the western part of Taiwan are nearly perpendicular to the major north-south highways. The Directorate General of Highways (DGH) in Taiwan had built many bridges across waterways over the past 60 years. These bridges often are subjected to threats imposed by the rivers with steep slope gradients and rapid flows during floods associated with typhoons, which are common from June—October. This often leads to bridge failures.

Considering the insufficient capacity for flood and the seismic resistance of these old bridges, the DGH had surveyed approximately 2,000 bridges nationwide during 2000–2007. Following the survey, the agency had identified 40 bridges in Taiwan as critical and placed them on a top-priority list for repair work. Ten of the 40 bridges have been considered extremely scour-critical and needed reconstruction immediately. In 2008, the DGH stated that repair works on these 10 bridges needed to be completed by 2013. Notwithstanding this, most of these extremely scour-critical bridges, which are at a high risk of collapse during floods, are still open to traffic. To ensure safety, however, the DGH has introduced plans to temporarily close these bridges on the basis of predetermined flood-warning levels during extreme weather conditions.

During Typhoon Sinlaku in September 2008, which pelted Taiwan with strong winds and heavy rain, six bridges collapsed and eight cars were buried by a landslide with a total casualty of seven deaths and 17 injuries. Among these six collapsed bridges, the Houfeng Bridge is one of the 10 extremely scour-critical bridges previously identified by the DGH. The Houfeng Bridge, which crosses the Da-Chia River in central Taiwan, collapsed at 6:50 pm on September 14, 2008.

Records have shown that the Houfeng Bridge was closed to traffic during Typhoon Fungwong (July 28, 2008), which occurred approximately 1.5 months before the present event; the bridge survived the July episode. During the September 14 event, the DGH similarly attempted to close the Houfeng Bridge on the basis of the same flood-warning level at 204.27 m above mean sea level (MSL), which is 1 m below the top of the caisson. Although one end of the bridge was closed, the authority was unable to prevent 3 vehicles from entering the bridge from the other direction. As a result, six lives were lost because the collapse of the bridge occured at the very moment when the vehicles arrived at the damaged section.

Fig. 1(a) shows the flow condition upstream of the Houfeng Bridge after recession of the flood on September 24, 2008. One may clearly deduce from the photograph in the figure that the direct cause of failure is the damage to Pier 2 (P2), close to the right bank of the river. The photograph also reveals the presence of an encased pipeline located approximately 20 m upstream of the bridge, which causes the formation of an impinging jet flow toward the bridge. Fig. 1(b), which is a photograph taken when the flood discharge was still high, evidently shows how the jet impinges directly onto the piers. It may be surmised that the impinging jet induced by the encased pipeline must have had a very important bearing on the eventual demise of the bridge. In addition, Fig. 1(a) also shows how the overall bed degradation associated with long-term general scour of the river bed had exposed the caisson, which forms the foundation of the bridge.

Fig. 2 shows the remnant of Pier 2; one may deduce from this figure that Pier 2 had collapsed toward the downstream direction,

[1]Postdoctoral Research Fellow, Dept. of Civil Engineering, National Chung Hsing Univ., Taichung 402, Taiwan.

[2]Professor, School of Civil and Structure Engineering, Nanyang Technological Univ., Singapore.

[3]Professor, Dept. of Civil Engineering, National Chung Hsing Univ., Taichung 402, Taiwan (corresponding author). E-mail: jylu@mail.nchu.edu.tw

[4]Research Fellow, Hydrotech Research Institute, National Taiwan Univ., Taipei 106, Taiwan.

[5]Research Fellow, National Center for Research on Earthquake Engineering, Taipei 106, Taiwan.

Note. This manuscript was submitted on September 23, 2009; approved on March 23, 2011; published online on March 24, 2011. Discussion period open until July 1, 2012; separate discussions must be submitted for individual papers. This paper is part of the ***Journal of Hydraulic Engineering***, Vol. 138, No. 2, February 1, 2012. ©ASCE, ISSN 0733-9429/2012/2-186–198/$25.00.

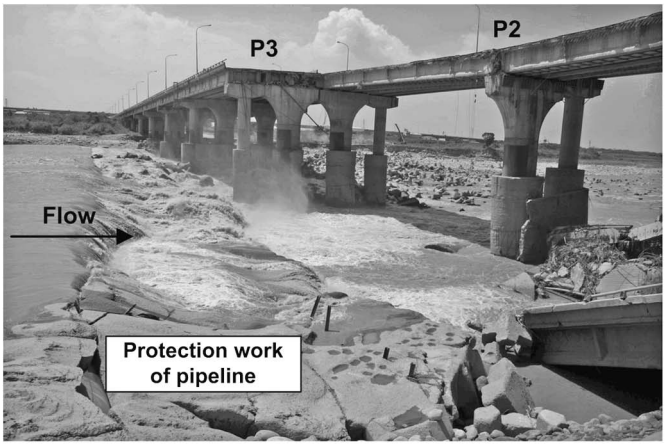

(a)

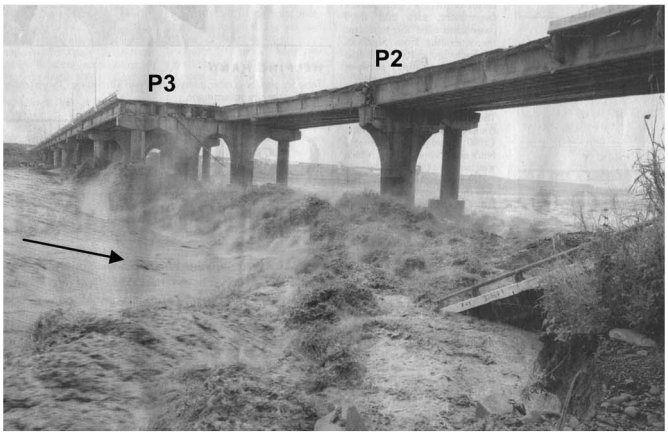

(b)

Fig. 1. Photographs of Houfeng Bridge: (a) flow field around Houfeng Bridge showing the presence of an upstream encased pipeline (Sept. 24, 2008); (b) impinging jet downstream of the encased pipeline at Houfeng Bridge (Sep. 15, 2008) (images by the authors)

Fig. 2. Remnant of Pier 2 after the failure of Houfeng Bridge (Oct. 2008) (image by the authors)

and that the toe of the caisson is unabridged. It indicates that the total scour depth during the flood must have undermined the caisson. Furthermore, the figure reveals that only a few concrete armoring units, which were designed as a scour countermeasure, had survived the flood during Typhoon Sinlaku. One may deduce from this evidence that the concrete armor units are ineffective in arresting scour, at least not for the condition experienced at the Houfeng Bridge.

The cause of the failure of the Houfeng Bridge is complex. Although the direct cause of failure may be attributed to local pier-scour, it is naïve to suggest that it is the only factor. On the basis of visual evidences and all available data before and during the flood, an attempt is put forward to offer an explanation on all contributing factors that led to the eventual failure of the bridge. It is hoped that with this forensic review of available information relating to the failure of the bridge, engineers will be better able to tackle bridge safety worldwide in general and particularly in Taiwan in the future. Moreover, an attempt is also made to evaluate the various scour depths, both general and local, associated with Pier 2 by using published scour formulas. This will allow us to have a clearer understanding of how each of these components contributed to the eventual undermining of the caisson. If such formulas are found to be accurate in determining the extent of scour, they may be used for future design of pier foundation in Taiwan with a higher degree of confidence.

Site Descriptions and Flow Information

The Houfeng Bridge, which was opened to traffic in 1990, is a four-lane, two-way, provincial highway 13 bridge that spans the Da-Chia River in central Taiwan. It connects the Houli township in the north and Fengyuan City in the south. The length of the bridge is 640 m with 16 spans. The superstructure consists of steel plate girders with a reinforced-concrete slab deck. Each pier consists of four 2-m-diameter reinforced-concrete cylinders tied with a reinforced-concrete capping beam. These circular piers were founded on cylindrical concrete caissons with diameter = 4 m and length = 14 m [see Fig. 1(a)]. All the caissons were originally designed to be completely embedded within the river bed.

The Da-Chia River Basin upstream of the Houfeng Bridge has a drainage area of 1,204 km^2. As the third longest river in Taiwan, the Da-Chia River, which has a total length of 124 km, flows westward for another 25 km from the Houfeng Bridge before reaching the Taiwan Strait. The tidal effect from the river mouth does not influence flows at the bridge. The Shihkang Dam, which was constructed in 1977 to supply water for domestic use in the central part of Taiwan, is located approximately 5 km upstream of the Houfeng Bridge. The aerial photograph in Fig. 3 shows the braided character of the Da-Chia River in the reach between the Houfeng Bridge and National Expressway No. 1 Bridge. According to surveys conducted by the Third River Management Office in Taiwan from 1999 to 2004, the thalweg of Da-Chia River in the reach near the Houfeng Bridge is generally located on the northern side of the river (right bank). The river approaches the bridge at an angle of 15° to the longitudinal axis of the bridge.

Bed samples obtained in the vicinity of the Houfeng Bridge has a median size (d_{50}) of approximately 80 mm and a geometric standard deviation (σ_g) of approximately 6.32. This shows that the bed sediments are small cobbles, and the sediment particles are poorly sorted.

Auxiliary Artificial Engineering Structures around Houfeng Bridge

A search through the records in engineering works carried out around the Houfeng Bridge reveals that three important auxiliary

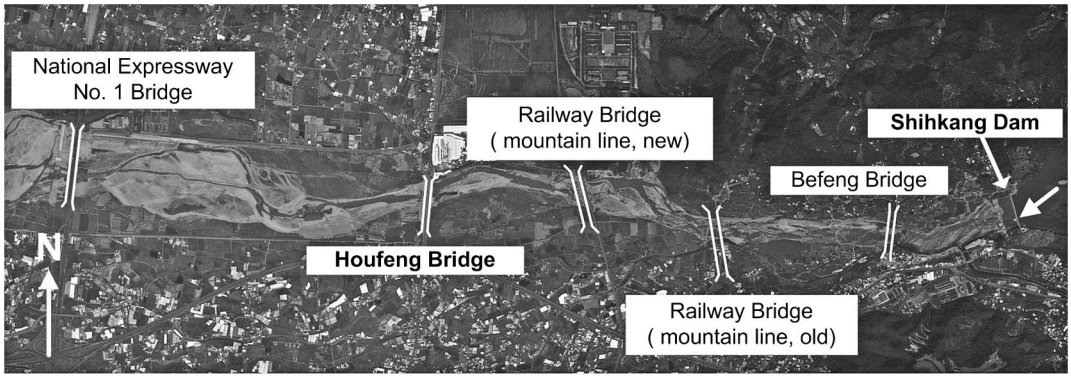

Fig. 3. Aerial photograph around Houfeng Bridge in 2007; flow is from right to left (image courtesy of the Shihkang Dam Water Resources Management)

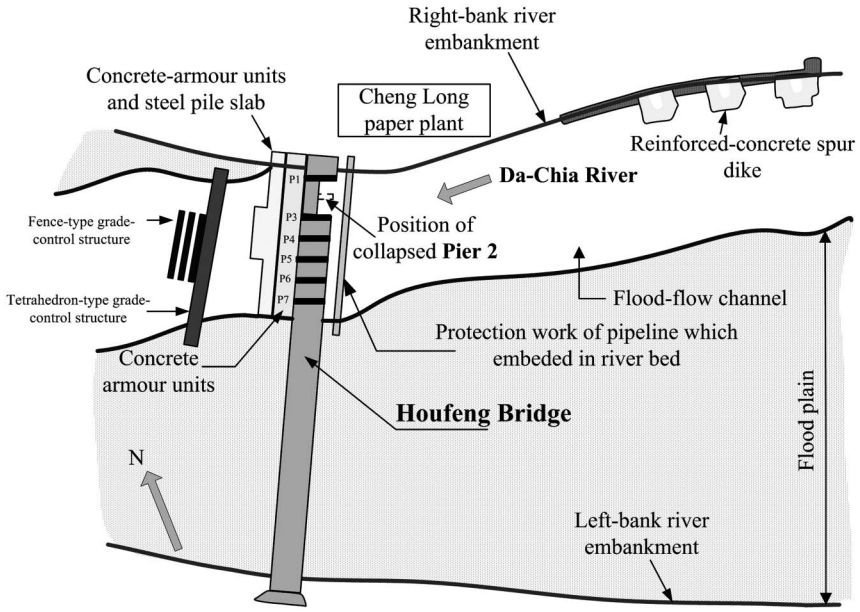

Fig. 4. Schematic site plan of the Houfeng Bridge near-field at failure

artificial structures were constructed before the demise of the bridge in September 2008. They are (1) an encased pipeline; (2) a tetrahedron type grade-control structure; and (3) a steel-fence type grade-control structure. The first one was located upstream; whereas, the others were located downstream of the bridge (see Fig. 4). It is envisaged that items (1) and (3) have an important influence in contributing to the eventual collapse of the bridge. The descriptions of and reasons for their construction are outlined as follows:

Encased Pipeline

As was discussed in the preceding section, photographs taken after the collapse of the Houfeng Bridge [see Fig. 1(a)] show the presence of an encased pipeline located just upstream of the bridge. Records show that the pipeline was originally constructed in 1994. Initially, the pipeline was embedded at a depth of 7 m beneath the river bed. During Typhoons Haitang and Matsa in 2005, extensive general scour took place along this reach of the river resulting in the exposure and partial suspension of the pipeline. Remedial work in encasing the pipeline was immediately carried out to prevent damage to the water supply line. The result is the construction of a concrete casing as a protective cover over the pipeline.

Grade-Control Structures

Typhoons Haitang and Matsa significantly exposed the foundation of Pier 2 in 2005. To protect the bridge, the DGH constructed a tetrahedron type grade-control structure at the location of approximately 60 m downstream of the Houfeng Bridge in 2007. Another three steel-fence type grade-control structures were independently constructed by the Third River Management Office approximately 80 m downstream of the Houfeng Bridge. Fig. 4 shows the location of both these grade-control structures. The latter grade-control structure, which is 81 m long, partially crosses the main channel. The collapsed Pier 2 was located in the main channel, which has a width of approximately 230 m. It is believed that the 81-m-long

grade-control structure downstream of the Houfeng Bridge may have caused contraction scour and head-cutting during high flow conditions.

Concrete Armor Units

To strengthen the extremely scour-critical Houfeng Bridge, the DGH had launched a lot of concrete armor units, such as tetrapods and cable-tied blocks, at the bridge sites before Typhoon Sinlaku. Placement of approximately 1,600 tetrapods was carried out on July 28, 2008 approximately 1.5 months before the collapse of the Houfeng Bridge. This was necessitated by the severe scouring at Piers 2 and 3 of the bridge caused by Typhoon Kalmaegi on July 18, 2008. Unfortunately, they were all found to be highly ineffective. Figs. 1(a) and 2 show how they were almost all washed away during the typhoon. This observation shows that this kind of concrete armor unit is ineffective in preventing scour during typhoon-induced floods for rivers with steep gradients in Taiwan.

Flow Information

A stream-gauging station situated at the Houfeng Bridge has an attached ultrasonic stage-gauge; this enables us to have an accurate record of the flood hydrograph before its demise. The hydrograph associated with the bridge failure is shown in Fig. 5. The water–stage hydrograph measured at the Houfeng Bridge during Typhoon Sinlaku (Sept. 14, 2008) is plotted with the corresponding flood discharge hydrograph measured at the Shihkang Dam, which is located approximately 5 km upstream of the bridge. Fig. 5 shows no record of the water-stage hydrograph after 6:45 pm on September 14, 2008 attributed to the collapse of the bridge. The data also show that the time of collapse coincides with the peak flow induced by Typhoon Sinlaku. On the basis of the 46-year records, the flood peak of 4,230 m^3/s in Typhoon Sinlaku is the 4th highest flood on record.

Major Events and Causes of the Collapse

An extremely important factor that has significantly contributed to the collapse of the Houfeng Bridge is the considerable bed degradation attributed to general scouring of the Da-Chia River. It is interesting to note that the Chi-Chi Earthquake, which took place on September 21, 1999, had a direct influence on long-term riverbed degradation, which in turn may have significantly contributed to the collapse of the bridge. The destructive Chi-Chi Earthquake, with a magnitude of 7.3 on the Richter scale, occurred in the center of Taiwan. The death toll in this catastrophe reached more than 2,000. Fig. 6(a) shows variations of the longitudinal riverbed profiles of the Da-Chia River from 1993 to 2008. The bed level reached a quasi-equilibrium condition over the period from 1993 to 1998. In 1999, nine years after the opening of the Houfeng Bridge, the Chi-Chi Earthquake occurred, resulting in the lifting of the surrounding ground levels along a fault line just upstream of the Shihkang Dam to create a 10-m drop in the Da-Chia River, as shown in Fig. 6(b). Over the subsequent years from 1999 to 2008, the Da-Chia River responded to this abrupt uplift through significant bed degradation in the river reach downstream of the dam. Coupled with this scour potential, the flood flows associated with typhoons have contributed to extensive general scour of the river. The combined effect of both these occurrences led to an average lowering rate of the river bed at the Houfeng Bridge of approximately 0.5 m/y or a total of 4.51 m over the past 9 years from 2008.

During Typhoon Mindulle in 2004, the mean riverbed and thalweg levels were lowered to approximately 200 and 195 m above the mean sea level (MSL) at the Houfeng Bridge, respectively. Thus, the extent of bed degradation has caused exposure of the caisson by a value of between 5.27 to 10.27 m because the top of the caissons level is at 205.27 m (MSL). Because the depth of the caisson is only 14 m, one can deduce that the Houfeng Bridge was already extremely vulnerable to scouring and failure 4 years before its final demise.

In 2005, Typhoons Haitang and Matsa caused considerable bed degradation, exposing the buried water supply pipeline just

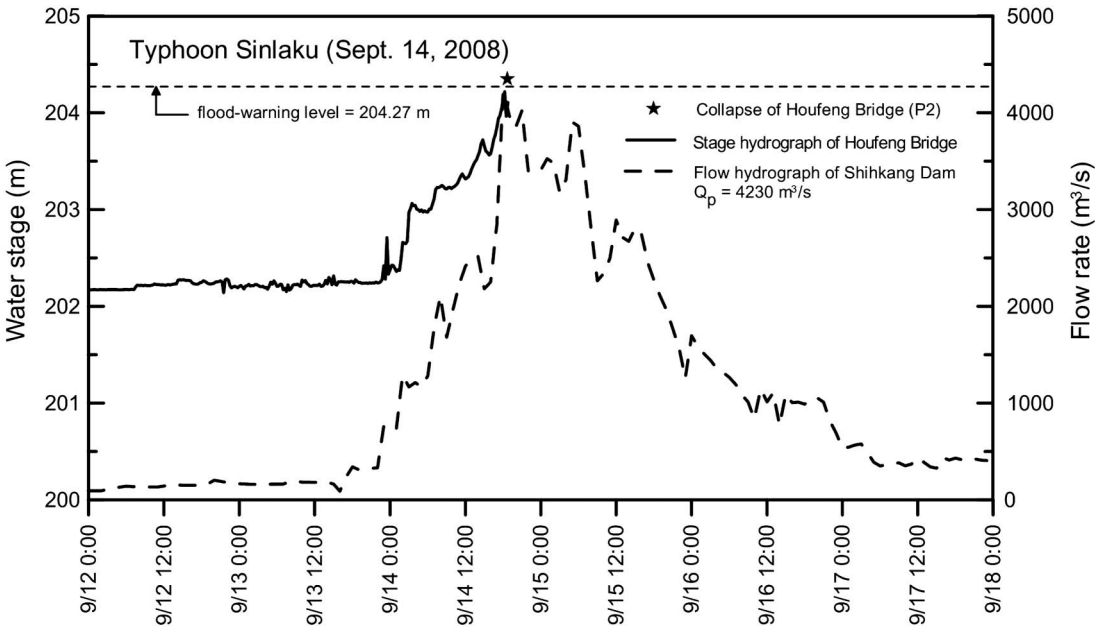

Fig. 5. Hydrograph at the Houfeng Bridge before its failure (data from Shihkang Dam and the Third River Management Office)

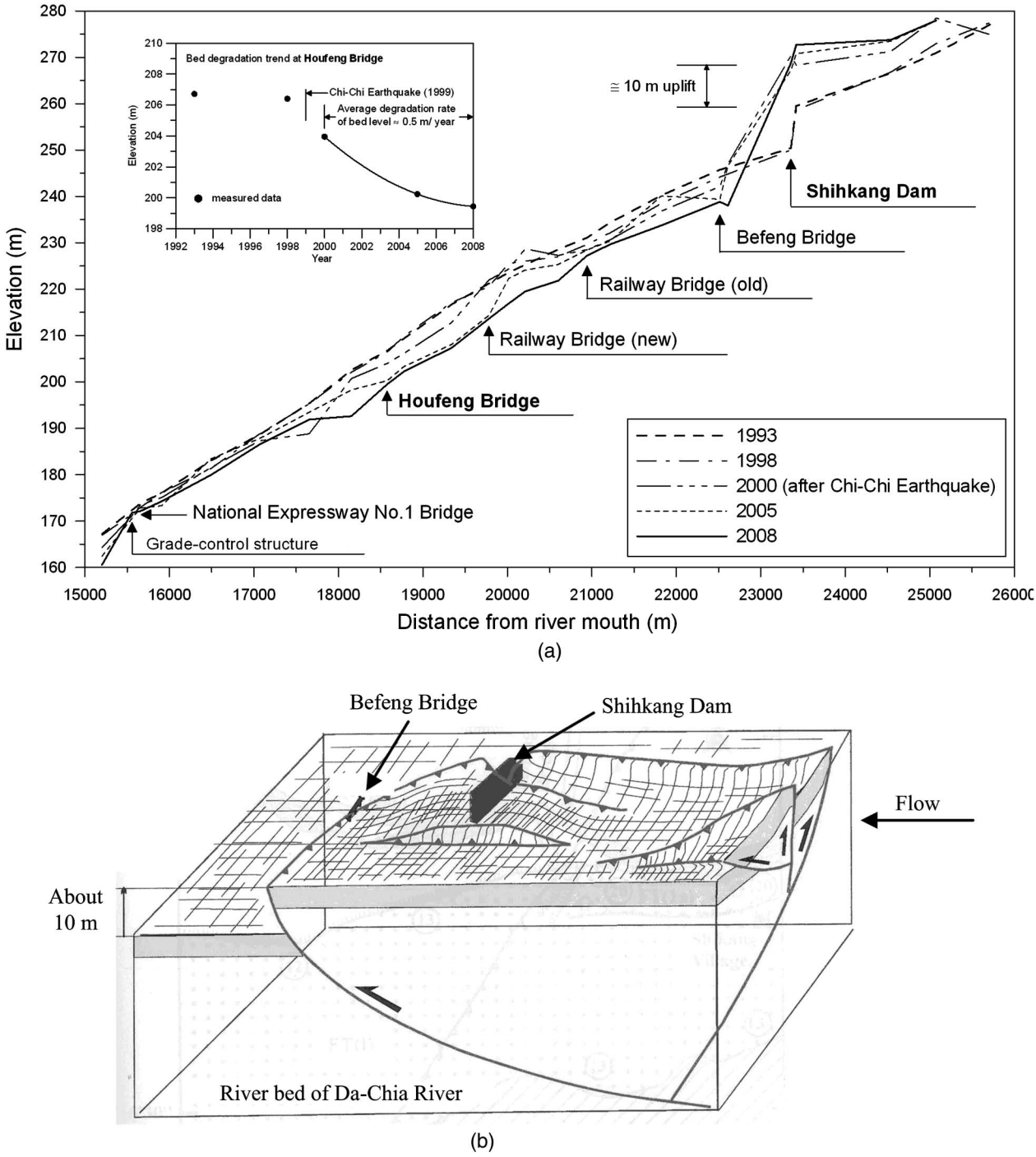

Fig. 6. Uplift of 10-m caused by the Chelongbu fault near Shihkang Dam: (a) variations of longitudinal riverbed profiles for Da-Chia River; (b) 3D schematic diagram showing the 10-m uplift caused by the Chelongbu fault near Shihkang Dam (courtesy of Yuan-Hsi Lee)

upstream of the Houfeng Bridge. In response to this perceived threat, the government built a downward-tilted casing over the pipeline (see Fig. 7). Unfortunately, this exposed structure upstream of the Houfeng Bridge dealt a further blow on the vulnerability of the bridge foundation. This is because the encased pipeline caused the formation of a strong impinging jet flow that impacted directly onto the foundation of the bridge.

Table 1 summarizes the major events relating to the failure of the Houfeng Bridge. Our analysis has found that many of these well-intended solutions may be either ineffective or counterproductive to improve bridge stability. In the next section, quantitative evaluation of scour depths relating to different scour processes will be given to confirm our hypotheses.

Analysis of Different Scour Components

Field evidences and thorough analysis of available data associated with the Houfeng Bridge reveal that failure of the bridge likely is attributed to undermining of the caisson connected to

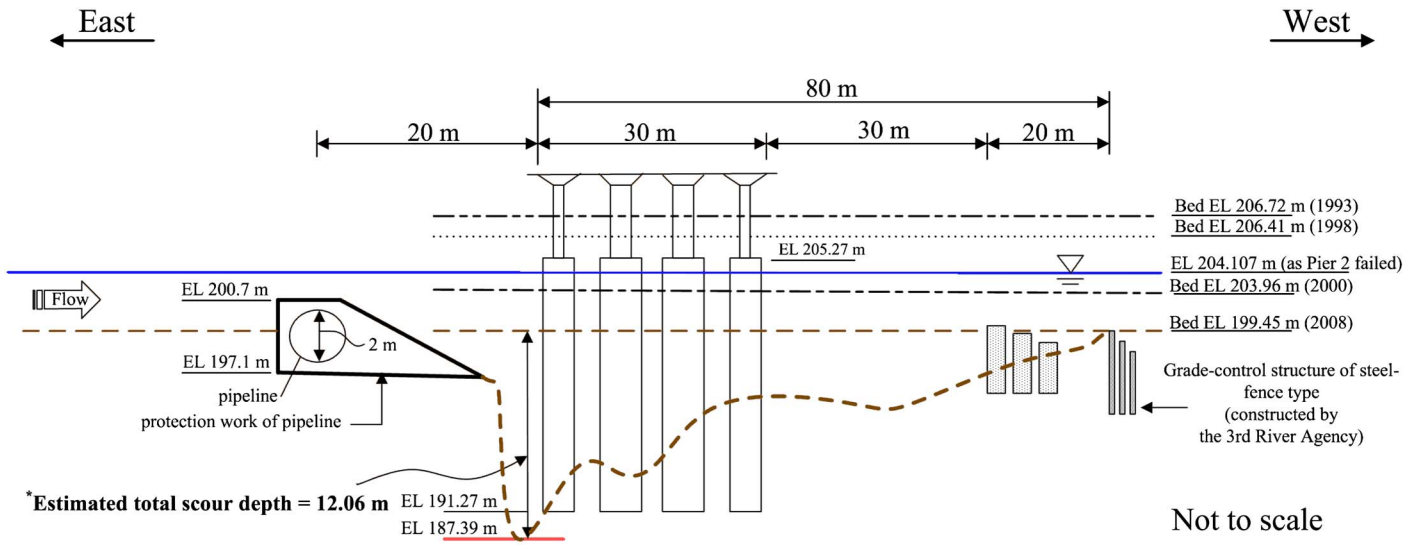

Fig. 7. Schematic diagram for the quantitative analysis of scour depth

Table 1. Major Events that Occurred in the Da-Chia River

Time	Events	Remark
1994	Water supply pipeline was constructed	The pipeline was embedded a depth of 7 m beneath the surface of river bed
September 21, 1999	Occurrence of Chi-Chi Earthquake	Magnitude 7.3 on the Richter scale was recoded and a lift of the river bed was up to approximately 10 m just upstream of the Shihkang Dam
2004	Thalweg lowered down to 195 m MSL at Houfeng Bridge during Typhoon Mindulle	The Directorate General of Highways placed the pier protection work
2005	Water supply pipeline exposed attributed to the flood events of Typhoons Haitang and Matsa	A protection work for the pipeline was constructed after the floods
April 2008	Three steel-fence type grade-control structures located approximately 80 m downstream of the Houfeng Bridge were constructed	Each one is 5-m-high, 3-m-deep, and 81-m-long
July 18, 2008	Foundations of Piers 2 and 3 of Houfeng Bridge were severely exposed during the flood event of Typhoon Kalmaegi	1,600 tetrapods were launched at piers to reduce the scour during the flood $Q_p = 3088$ m^3/s
6:50 pm, Sept. 14, 2008	Officers started to block off Houfeng Bridge collapse of Pier 2 after blockade of one end of the Houfeng Bridge	$Q_p = 4230$ m^3/s Three cars fell into the Da-Chia River, six people died

Pier 2 (P2). Hence, it is reasonable to surmise that the total depth of scour at this location must have at least approached the embedment depth of the caisson, which is at 191.27 m MSL (the caisson top level = 205.27 m MSL; the depth of caisson = 14 m). Examinations of all the events before and during the flood associated with Typhoon Sinlaku show that the total scour depth is a combination of the following scour depths: (1) general scour, both long-term and short-term; (2) contraction scour depth; (3) bend scour depth; (4) pier-scour depth; and (5) impinging jet scour depth. The overall effect of these interrelated scour processes is a very complex phenomenon. So far, interactions of the processes of general scour, contraction scour, bend scour, local

Table 2. Bed Degradation Downstream of the Shihkang Dam in Da-Chia River after the Chi-Chi Earthquake from 1999 to 2008

Site	Distance to Shihkang dam (km)	Degradation between 1993 to 1999 (m)	Degradation between 1999 to 2008 (m)	Average degradation rate between 1993 to 1999 (m/year)	Average degradation rate between 1999 to 2008 (m/year)
Befeng Bridge	0.84	1.55 (245.75 – 244.2)	3.31 (242.15 – 239.38)	0.26	0.37
Railway Bridge (old)	2.41	1.45 (231.1 – 229.65)	1.28 (228.52 – 228.47)	0.24	0.14
Railway Bridge (new)	3.58	0.64 (221.21 – 220.57)	8.35 (221.97 – 214.32)	0.11	0.93
Houfeng Bridge	4.78	0.31 (206.72 – 206.41)	4.51 (203.96 – 200.24)	0.05	0.50
National Expressway No.1 Bridge	7.70	0.86 (173.78 – 172.92)	1.31 (172.78 – 172.13)	0.14	0.15

Note: Numbers within (…) are referenced from the mean sea levels. The above data were reported by the Water Resources Planning Institute (2008).

scour, and impinging jet scour are unknown. Federal Highway Administration guidelines (Richardson and Davis 1995) and bridge scour texts, such as Melville and Coleman (2000), recommended that all the components of scour depths may be assumed to be independent. On the basis of this assumption, the total depth of scour at the bridge is then simply the sum of all the scour components to provide a conservative estimate. In this section of the paper, an attempt is made to compute the total depth of scour at the pier by independently evaluating each of these scour depths by using published formulas. All the formulas used in this paper are listed in the appendix.

General Scour

General scour, which occurs irrespective of the presence of a hydraulic structure, such as a pier, is defined as the continuous lowering of the river bed with time. It may be in the form of long-term (bed degradation) or short-term general scour. The former occurs over a considerabe length of time, normally in the order of several years or longer; whereas the latter occurs during floods (Melville and Coleman 2000). Measured field data show that the Houfeng Bridge experienced both these types of scour.

Long-Term General Scour (Bed Degradation)

Table 2 shows the extent of bed degradation downstream of the Shihkang Dam before and after the Chi-Chi Earthquake. Before the earthquake from 1993 to 1998, a total of approximately 0.3 m of bed degradation had taken place in the vicinity of the Houfeng Bridge, and the caisson remained buried below the river bed by 1.14 m (river bed level = 206.41 m MSL, the caisson top level = 205.27 m MSL) in 1998. Lifting of the river bed along the fault at the Shihkang Dam created a 10-m drop during the earthquake and steepened the channel slope resulting in a substantial increase of bed material discharge. This effect progresses in the downstream direction, leading to severe lowering of the bed of the Da-Chia River with an average of 8.35 m at the location 3.58 km downstream from the Shihkang Dam over the next 9 years from 1999 to 2008. The total bed degradation at the Houfeng Bridge site was recorded at 4.51 m in 2008. Fig. 7 shows how this severe bed degradation has caused the caisson at Pier 2 to protrude above the mean river bed level, which was at 199.45 m MSL. The field data in Table 2 also show how the bed degradation rate of the Da-Chia River is significantly affected by the Chi-Chi Earthquake, with the postearthquake bed degradation rate close to one order of magnitude larger than its preearthquake counterpart. For example, the respective rates of degradation are 0.93 versus 0.11 mm/y at the new Railway Bridge and 0.50 versus 0.05 m/y at the Houfeng Bridge.

The extent of bed degradation, regarded as long-term general scour depth of 4.51 m at the Houfeng Bridge from 1999 to 2008, is not directly related to Typhoon Sinlaku. It is a response of the river to the cumulative effect of the Chi-Chi Earthquake and all

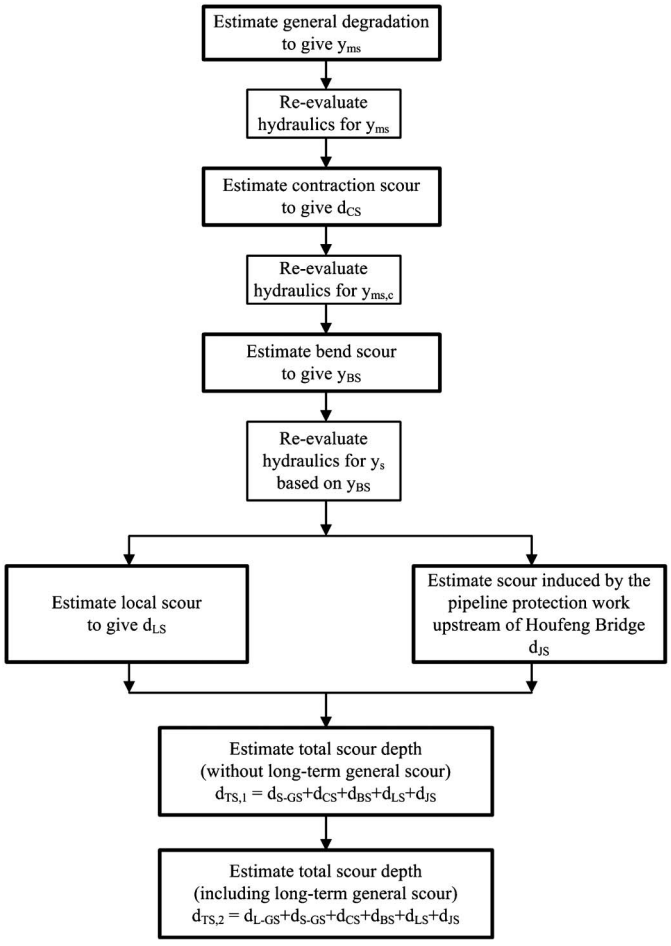

Fig. 8. Methodology for quantitative prediction of scour depth (modification of method proposed by Melville and Coleman 2000)

Table 3. Basic Data for the Scour Analysis of Houfeng Bridge

Category	Basic data	Typhoon Sinlaku (Sept. 14, 2008)
Channel	Channel centre-line radius of curvature r_c (m)	2,870
	Channel slope S_b	0.011
	Channel width W (m)	230
Flow	Flow discharge Q (m^3/s)	4,230
	Average upstream unscoured flow depth y_u (m)	4.657
	flood peak duration t (days)	0.0625
Bed material	Median size d_{50} (mm)	80
	d_{90} (mm)	230
	Geometric standard deviation σ_g	6.32
	Specific gravity G_s	2.65
Bridge	Bridge length (m)	640
	Number of piers	15
	Bridge span (m)	40
	Pier width b (m)	2
	Caisson width b^* (m)	4
	Caisson depth L_c (m)	14
	Angle of attack θ (degree)	15
Protection work of pipeline	Downstream slope of protection work S_{rm} (V:H)	0.31
Grade-control structure	Length of grade-control structure L_g (m)	81
Elevation	Water-stage as pier failed EL_{wf} (m)	204.107
	Caisson top level (in main channel) EL_c (m)	205.27
	Caisson toe level EL_{ct} (m)	191.27
	Top level of pipeline protection work EL_p (m)	200.70
	Flood-level warning I EL_{fwI} (m)	204.27

Table 4. Evaluation of the Degraded Channel Section

Scour analysis	Pier 2
Flow depth after degradation y_{ms} (m)	
Lacey (1930), from (1) & (2)	(3.03)[a]
Blench (1969), from (3) & (4)	5.95
Maza Alvarez and Echavarria Alfaro (1973), from (5)	5.32
Averaged value of y_{ms} (m)	5.64

[a]Lacey's (1930) method was disregarded because the y_{ms} value is less than the upstream unscoured flow depth y_u.

preceding Typhoon-induced floods. Notwithstanding the severity of this effect, it still is unable to undermine the caisson attached to Pier 2 of the Houfeng Bridge. Its final demise must, therefore, be related to the Typhoon Sinlaku-induced flood on September 14, 2008. In the next section, each of the scour components is computed by using the available information and actual flood data.

Evaluation of Scour Depth Induced by Typhoon Sinlaku

Melville and Coleman (2000) proposed a methodology to calculate scour depths quantitatively. In this paper, their method is adopted and modified as shown in Fig. 8 to evaluate the scour depth. Table 3 summarizes all relevant data needed for the scour calculation.

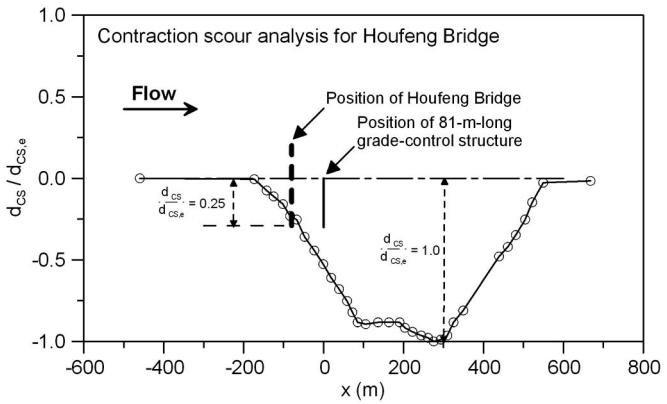

Fig. 9. Bed profile under long-contraction scour condition for an opening ratio of 0.6

Short-Term General Scour

The short-term general scour depth is assumed to be directly related to the peak flood associated with Typhoon Sinlaku on Sept. 14, 2008. Melville and Coleman (2000) have proposed three methods (see the appendix) for the computation of scoured flow depth during floods. By using these methods, the results, which were computed by using the peak-flow condition, are tabulated in Table 4. The average scoured flow depth of 5.63 m is calculated by using the relationships proposed by Blench (1969) and Maza Alvarez and Echavarria Alfaro (1973). The value, based on Lacey's (1930) method, was disregarded because the y_{ms}-value is less than the upstream unscoured flow depth y_u, and the size of the sediment particles of the Da-Chia River is markedly more than that recommended by this approach.

Contraction Scour

Published methods for estimating contraction scour (e.g., Laursen 1960) are generally based on theoretical analyses of experimental study in a long rectangular contraction. However, in this study, the contraction scour induced by the 81-m-long grade-control structure downstream of the Houfeng Bridge is very different from a long-contraction scour, with the contraction ratios ($\beta = W_1/W_2$) at the Houfeng Bridge and grade-control structure being 1.14 and 1.54, respectively, where W_1 and W_2 = widths of the uncontracted and bridge (or contracted) sections, respectively. As far as the authors are aware, few laboratory or field measurements are available for estimating this kind of contraction scour depth.

Recently, Dey and Raikar (2005) investigated long-contraction scour and bed variation in the streamwise direction under clear-water scour conditions. After adjusting the flow conditions for general scour, the average flow intensity V/V_c calculated from the formulas of Raudkivi (1990) and Neill (1968) is 1.07, which is close to 1.0. On the basis of Laursen's (1960) equation and Dey and Raikar's (2005) experimental results, the long-contraction scour depth and the ratio of the contraction scour depth at Pier 2 to equilibrium contraction scour depth $d_{sc}/d_{sc,e}$ are estimated to be 2.08 and 0.25—(Fig. 9), respectively. On the basis of this calculation, the contraction scour depth at Pier 2 is found to be 0.52 m. It must

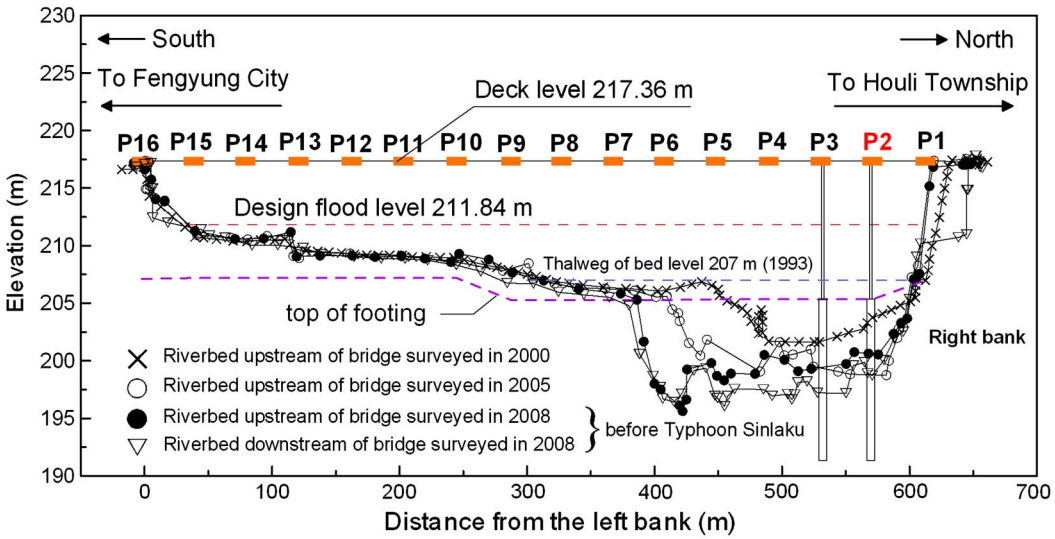

Fig. 10. Cross-sectional variations of Da-Chia River near the Houfeng Bridge

Table 5. Evaluation of Degraded Channel Section at Houfeng Bridge

Scour analysis	Calculated value
Degraded channel section	
Flow depth y_{ms} (m) (from Table 4)	5.64
Average velocity V (m/s)	3.26
Critical velocity for sediment entrainment V_c (m/s), from (6) & (7)	3.06
Flow depth after contraction scour by downstream 81-m-long grade-control structure $y_{ms,c}(\equiv \mathbf{y}_{ms} + d_{CS})$ (m), from (8)	6.16
Flow depth after bend scour y_{BS} (m)	
Lacey I (1930), from (10)	(12.32)[a]
Lacey II (1930), from (11)	7.66
Chatley (1931), from (12)	5.35
Thorne (1988), from (13)	7.56
Averaged y_{BS} value	6.86
Scoured flow depth at the given foundation $y_s = y_{BS}$	6.86

[a]Discarded.

Table 6. Evaluation of Local Scour at Pier 2 of Houfeng Bridge

Scour parameter	Calculated value
Scoured channel section	
Flow depth approaching pier y_s (m) (from Table 5)	6.86
Flow velocity at pier $V = q/y_s$ (m/s)	2.68
Critical velocity V_c (m/s)	3.76
Caisson top level Y (m)	−5.82
Local pier-scour	
Pier width b (m)	2.00
Caisson width b^* (m)	4.00
Equivalent pier width b_e (m)	3.81
Flow depth pier size factor k_{yb} (m)	9.14
Median size of armor layer d_{50a} (m)	0.13
Critical stress for armor layer θ_{ca}	0.056
Armoring critical velocity V_{ca} (m/s)	4.39
"Armor peak" flow velocity V_a (m/s)	3.51
Flow intensity factor K_I	0.78
Sediment size factor K_d	1.04
Foundation shape factor K_s	1.0
Pier length l (m)	4.0
Foundation alignment to flow $\theta(°)$	15
Foundation alignment factor K_θ	1.15
Channel geometry factor K_G	1.0
Time for equilibrium scour t_e (days)	21.54
Time factor K_t	0.74
Local pier-scour depth d_{LS} (m), from (14)	6.34
Jet scour induced by the protection work of pipeline d_{JS} (m), from (27)	3.52

be stated that the computed value likely does not give an accurate answer to what actually transpired because the field condition does not satisfy the long-contraction assumption of the proposed equation. However, because the method for computing such a short contraction remains elusive presently, a first-order estimate by using the long-contraction method is adopted. Such an approach likely is conservative, and because it is shown later that the contribution of contraction scour, even in using the conservative long-contraction scour equation, only contributes to 3% of the overall depth of scour, its role in affecting the stability of the Houfeng Bridge is insignificant.

Bend Scour

Fig. 3 shows how the Houfeng Bridge is located at a mild right-hand bend of the Da-Chia River and the river approaches the bridge at an angle of 15° to the longitudinal axis of the bridge. Fig. 10, which contains the cross-sectional variations of the Da-Chia River near the Houfeng Bridge, clearly shows that five piers are located within the main channel (P2-P6) at the northern end of the bridge. According to surveys conducted by the Water Resources Planning Institute between the Chi-Chi Earthquake and Typhoon Sinlaku (from 2000 to 2008), both the width of the main channel and the lowering of the thalweg increased with time.

Computation of bend scour was conducted by using four different approaches: Chatley (1931); Thorne (1988); and two simple graphical solutions proposed by Lacey (1930), conveniently denoted as Lacey I and Lacey II (see the appendix). The calculated results using all these methods are tabulated in Table 5.

Table 5 shows that the bend scour depth estimated by using the method of Lacey I is 12.32 m with the corresponding bed levels at 191.79 m MSL. This value is less than the bed level (197.1 m MSL) on which the encased pipeline is resting. If bend scour had in fact caused such an extensive erosion (in the order of 5 m), the concrete pipeline-casing likely would have cracked. Because field observations after the flood did not show such an occurrence, the computed bend scour depth using Lacey I probably is too excessive. For this reason, the method of Lacey I is discarded from further analyses. The results from the calculations conducted by using the methods of Thorne (1988), Lacey II (1930), and Chatley (1931) are 7.56, 7.66 and 5.35 m, respectively; they yield a more reasonable average maximum bend scour depth of 6.86 (y_{BS}) or 197.25 m MSL. Table 5 summarizes all the data needed for the computation of bend scour depth at the Houfeng Bridge and results.

Local Pier and Jet Scour

The scour relationship proposed by Melville and Coleman (2000) was used to calculate the local pier-scour depth, whereas the jet scour formula proposed by Bormann and Julien (1991) was used to compute the jet scour depth induced by the upstream encased pipeline. Assuming that critical flow will occur near the top of the encased pipeline and on the basis of the peak-flow unit discharge, the critical flow depth can be estimated by using $y_c = (q^2/g)^{1/3}$, q = unit flow rate; and g = gravitational acceleration, giving a value of $y_c = 3.25$ m. It may be surmised that the water surface elevation near the encased pipeline was 203.95 m MSL because the top elevation of the encased pipeline was 200.7 m MSL (see Fig. 7). Because the ultrasonic water-stage was installed at the downstream side of the Houfeng Bridge, it is believed that the flow condition of the impinging jet flow can be assumed to be a submerged flow condition. On the basis of the analysis, the formula proposed by Bormann and Julien (1991) was adopted to estimate the jet scour depth near the bridge.

Table 6 shows the results obtained for both the scour depths related to the bridge pier and impinging jet. The former is found to be 6.34 m and the latter 3.52 m.

Table 7 summarizes all the computed scour depths in the study. First of all, the results show that the total depth of scour (without long-term general scour) is 12.06 m. With the addition of the long-term general scour depth of 4.51 m over the past 9 years since the

Table 7. Comparison of Scour Components Calculated by the Proposed Methodology

Scour components			Ratio of scour components to total scour			
			Without bed degradation		Including bed degradation	
Long-term generalscour depth	$d_{L\text{-GS}}$ (m)	4.51	—	—	$d_{L\text{-GS}}/d_{\text{TS},2}$	0.27
Short-term generalscour depth	$d_{S\text{-GS}}$ (m)	0.98	$d_{S\text{-GS}}/d_{\text{TS},1}$	0.08	$d_{S\text{-GS}}/d_{\text{TS},2}$	0.06
Contraction scour depth	d_{CS} (m)	0.52	$d_{\text{CS}}/d_{\text{TS},1}$	0.04	$d_{\text{CS}}/d_{\text{TS},2}$	0.03
Bend scour depth	d_{BS} (m)	0.70	$d_{\text{BS}}/d_{\text{TS},1}$	0.06	$d_{\text{BS}}/d_{\text{TS},2}$	0.04
Local scour depth	d_{LS} (m)	6.34	$d_{\text{LS}}/d_{\text{TS},1}$	0.53	$d_{\text{LS}}/d_{\text{TS},2}$	0.38
Jet scour depth	d_{JS} (m)	3.52	$d_{\text{JS}}/d_{\text{TS},1}$	0.29	$d_{\text{JS}}/d_{\text{TS},2}$	0.21
Total scour depth without Long-term generalscour depth	$d_{\text{TS},1}$ (m)	12.06	$d_{\text{TS},1}/d_{\text{TS},1}$	1.00	$d_{\text{TS},2}/d_{\text{TS},2}$	1.0

Note: Bed degradation from 1999 to 2008 in the vicinity of Houfeng Bridge, $d_{L\text{-GS}} = 4.51$ m $d_{\text{TS},1} = d_{S\text{-GS}} + d_{\text{CS}} + d_{\text{BS}} + d_{\text{LS}} + d_{\text{JS}}$ (without long-term general scour), from (28) $d_{\text{TS},2} = d_{L\text{-GS}} + d_{S\text{-GS}} + d_{\text{CS}} + d_{\text{BS}} + d_{\text{LS}} + d_{\text{JS}}$ (including the long-term general scour), from (29).

Chi-Chi Earthquake, the total scour depth at Pier 2 of the Houfeng Bridge (P2) is a whopping 16.57 m! This value confirms the hypothesis that undermining of the caisson at Pier 2 is completely plausible because it is 3.88 m below the bottom of the caisson level. This undermining is, to a large extent, confirmed by field evidences at the bridge site after the flood. Considering only the total scour depth without contribution from long-term general scouring, the results reveal that local pier-scour contributes 53% of the overall scouring at the pier-caisson, while the short-term general scour (8%), contraction scour (4%), bend scour (6%), and impinging jet scour (29%) combine to contribute the remaining 47%. The data also show that the impinging jet generated by the encased pipeline had contributed significantly to the overall scour at the pier. This issue must be addressed if the Houfeng Bridge were to be rebuilt at its present location.

Additionally, if long-term general scour (bed degradation = 4.51 m) from 1999 to 2008 are included in the consideration, the total scour depth ($d_{\text{TS},2}$) at Pier 2 is 16.57 m. Approximately 27% of the total scour depth is attributed to long-term general scour of the Da-Chia River around the Houfeng Bridge, whereas the short-term general scour (6%), contraction scour (3%), bend scour (4%), local pier-scour (38%), and the impinging jet scour (21%) contribute to the remaining scour.

Conclusions and Recommendations

Proper prediction of the bridge scour, design of countermeasures and appropriate bridge closure are vital to avoid collapse of bridges or loss of lives. The collapse of the Houfeng Bridge was an important event in the development of bridge inspection and closure procedures in Taiwan. By using available data obtained before, during, and after the collapse of the Houfeng Bridge, a thorough forensic analysis is conducted and the following conclusions are drawn and recommendations proposed:

1. The study reinforces the fact that failure of a bridge often is attributed to multiple causes rather than pier-scour alone. This case study of the Houfeng Bridge reveals that its failure is related to long-term and short-term general scour of the river bed, contraction, bend, pier, and jet scour. Some of these causes are man-induced and the others are attributed to natural causes in the form of typhoon-induced floods and earthquake-induced bed degradation.
2. The destructive Chi-Chi Earthquake (7.3 on the Richter scale) has a significant long-term effect on bed degradation downstream of the Shihkang Dam. Analyses of field data with consideration of long-term general scour caused by the Chi-Chi Earthquake show that approximately 27% of the total scour depth at the bridge site is attributed to long-term general scour of the Da-Chia River. The short-term general scour (6%), contraction scour (3%), bend scour (4%), pier-scour (38%), and impinging jet scour (21%) combine to contribute the remaining 73%. The data reveal that the earthquake-induced bed degradation has contributed significantly to the overall scour at the pier. In addition, the channelization caused by the bed degradation had further enhanced exposure of the pipeline resulting in the severe jet scour.
3. The long-term general scour rate in a river, whether it is attributed to seismic or flood origin, must be evaluated through annual cross-section surveys or the conduct of numerical models; moreover, proper precautions must be taken if damage to or failure of hydraulic structures, in the vicinity of the bridge structure under observation, is identified.
4. The study shows that different government agencies must cooperate to deal with the problem. The failure of the Houfeng Bridge highlights the potential risk associated with human interventions, e.g., construction of the encased pipeline and grade-control structures to the overall bridge stability.
5. With proper modifications, quantitative analysis of the Houfeng Bridge by using Melville and Coleman's (2000) method provides reasonable estimates for various scour components in such a complex physical system; however, this is only one case study, and more field data are needed to evaluate its general applicability. Moreover, scouring processes are time dependent. In this case study, the time effect was simplified on the basis of the Melville and Coleman (2000) method. It is proposed that further studies on the temporal variation of scour depth under unsteady flow conditions be conducted to improve the reliability and accuracy of the prediction method.
6. One of the key lessons learned from this case study is the importance of bridge operation. Bridge closure should not simply be based on a fixed flood-warning level; variations of the scour depth or bed level during floods also need to be considered. Because natural rivers have a movable bed, the flood-warning level for extremely scour-critical bridges should be reevaluated after each flood event on the basis of site inspection. Furthermore, river bed monitoring technologies need to be improved, especially under high flood flows.

Appendix. Formulas for Different Scour Components

The formulas used for calculating the various scour components in the paper are given in this appendix. The methodology for the calculation of scour depths is illustrated in Fig. 8. Basic data for the scour analysis of the Houfeng Bridge are given in Table 3.

General Degradation

Lacey (1930)

$$f = 1.76 d_m^{0.5} \tag{1}$$

$$y_{ms} = 0.47(Q/f)^{1/3} \tag{2}$$

Blench (1969)

$$y_{ms} = 1.20(q^{2/3}/d_{50}^{1/6}), \qquad 0.06 < d_{50}(\text{mm}) \le 2.0 \tag{3}$$

$$y_{ms} = 1.23(q^{2/3}/d_{50}^{1/12}), \qquad d_{50}(\text{mm}) > 2.0 \tag{4}$$

The units of y_{ms}, q and d_{50} are m, $\text{m}^3/\text{s/m}$, and mm, respectively.

Maza Alvarez and Echavarria Alfaro (1973)

$$y_{ms} = 0.365\left(\frac{Q^{0.784}}{W^{0.784} d_{50}^{0.157}}\right) \tag{5}$$

Revised Flow Conditions for y_{ms}

$A = W y_{ms}$; $V = Q/A$; $R = W y_{ms}/(W + 2y_{ms})$ (assuming rectangular channel).

$$V_c = 5.75 u_{*c} \log(5.53 y_{ms}/d_{50}) \text{ (Raudkivi 1990)} \tag{6}$$

$$V_c = 5.67 y_{ms}^{1/6} d_{50}^{1/3} \text{ (Neill 1968)} \tag{7}$$

u_{*c} is determined from the Shields diagram. The average critical velocity is determined from Raudkivi's (1990) and Neill's (1968) equations.

Contraction Scour

Laursen (1960)

$$\frac{y_{ms} + d_{cs,e}}{y_{ms}} = \left(\frac{W_1}{W_2}\right)^{k_1} \tag{8}$$

$d_{CS} = d_{CS,e} \times K_{CS}$, K_{CS} is determined from Fig. 10, where W_1 and W_2 are the approach channel width and the clear opening width at the bridge, respectively; k_1 is determined based on u_*/ω; ω = fall velocity of sediment particles. In this study, the value of k_1 is 0.64 (for the condition with some suspended sediment transport).

Revised Flow Conditions for $y_{ms;c}$

$$y_{ms,c} = y_{ms} + d_{CS} \tag{9}$$

Bend Scour

Lacey I (1930)

$$y_{BS} = 2y_{ms} \tag{10}$$

where $y_{ms} = y_{ms,c}$.

Lacey II (1930)

$$y_{BS} = y_u + 2(y_{ms} - y_u) \tag{11}$$

where $y_{ms} = y_{ms,c}$.

Chatley (1931)

$$\frac{y_{BS}}{y_u} = 1 + 2(W/r_0) \tag{12}$$

where r_0 = the outer radius of the bend W = channel width.

Thorne (1988)

$$\frac{y_{BS}}{y_u} = 2.07 - 0.19 \ln[(r_c/W) - 2] \qquad \text{for } r_c/w > 2 \tag{13}$$

Revised Flow Conditions for y_{BS}

y_{BS}

Local-Pier Scour

Melville and Coleman (2000)

$$d_{LS} = K_{yb} K_I K_d K_s K_\theta K_G K_t \tag{14}$$

Flow Depth Foundation Size Factor K_{yb}

$$b_e = b\left(\frac{y_s + Y}{y_s + b^*}\right) + b^*\left(\frac{b^* - Y}{b^* + y_s}\right) \tag{15}$$

$$K_{yb} = 2.4 b_e \quad \text{for } b_e/y_s < 0.7 \tag{16a}$$

$$K_{yb} = 2\sqrt{y_s b_e} \quad \text{for } 0.7 < b_e/y_s < 5 \tag{16b}$$

$$K_{yb} = 4.5 y_s \quad \text{for } b_e/y_s > 5 \tag{16c}$$

Method of estimation: $b_e = b^*$ for b^* uniform over the scoured flow depth (y_s) at the pier; $b_e = b$ for b uniform over the scoured flow depth (y_s) at the pier; b_e = width of an equivalent uniform pier; Y = level of the top of caisson measured from undisturbed sediment bed (positive downwards).

Flow Intensity Factor K_I

$$K_I = \frac{V - (V_a - V_c)}{V_c} \quad \text{for } [V - (V_a - V_c)]/V_c < 1 \tag{17}$$

$$K_I = 1.0 \quad \text{for } [V - (V_a - V_c)]/V_c \ge 1 \tag{18}$$

Method of estimation: For uniform sediment: $d_{50a} \equiv d_{50}$ and $V_a \equiv V_c$; For nonuniform sediment: $d_{50a} = d_{\max}/1.8 \approx d_{84}/1.8 = \sigma_g d_{50}/1.8$; $V_a = 0.8 V_{ca}$, where V_{ca} is calculated for d_{50a} using $\theta_{ca} = u_*^2/(\Delta g d_{50a})$; and $V_c = 5.75 u_{*c} \log(5.53 y/d_{50})$ (Raudkivi 1990), where Δ = relative density $(-) = \frac{\rho_s}{\rho} - 1$.

Sediment Size Factor K_d

$$K_d = 0.57 \log\left(2.24 \frac{b_e}{d_{50a}}\right) \quad \text{for } b_e/d_{50a} \le 25 \tag{19}$$

$$K_d = 1.0 \quad \text{for } b_e/d_{50a} > 25 \tag{20}$$

Foundation Shape Factor K_s

$K_s = 1.0$ for a circular pier shape. Value of K_s appropriate to the piers are defined by Melville and Coleman (2000).

Foundation Alignment Factor K_θ

$$K_\theta = 1.0 \quad \text{for circular piers} \tag{21}$$

$$K_\theta = \left(\frac{l}{b_e}\sin\theta + \cos\theta\right)^{0.65} \quad \text{for noncircular piers} \tag{22}$$

Approach Channel Geometry Factor K_G

$K_G = 1.0$ if values of y_s and V are selected to be representative of the flow approaching the particular pier.

Time Factor K_t

$$K_t = 1.0 \quad \text{for } V/V_c \ge 1.0 \quad (d_{\text{LS}} \text{ developing rapidly forlive-bed conditions}) \tag{23}$$

$$K_t = \exp\left\{-0.03\left|\frac{V}{V_c}\ln\left(\frac{t}{t_e}\right)\right|^{1.6}\right\} \quad \text{for } V/V_c < 1.0 \tag{24}$$

$$t_e(\text{days}) = 48.26 \frac{b_e}{V}\left(\frac{V}{V_c} - 0.4\right) \quad \text{for } y_s/b_e > 6, \quad V/V_c > 0.4 \tag{25}$$

$$t_e(\text{days}) = 30.89 \frac{b_e}{V}\left(\frac{V}{V_c} - 0.4\right)\left(\frac{y_s}{b_e}\right)^{0.25} \quad \text{for } y_s/b_e > 6, \quad V/V_c > 0.4 \tag{26}$$

Impinging Jet Scour

Boremann and Julien (1991)

$$d_{\text{JS}} + D_P = \frac{K_b q^{0.6} V_1 \sin\theta}{(2\Delta g)^{0.8} d_{90}^{0.4}} \tag{27}$$

where D_P = drop height of grade-control structure (m); g = acceleration of gravity, $g = 9.81$ m/s^2; K_b = coefficient (-) V_1 = jet velocity entering tailwater (m/s); Δ = relative density $(-) = \frac{\rho_s}{\rho} - 1$; θ = jet angle near surface.

Total Scour at the Pier

$$d_{\text{TS},1} = d_{S\text{-GS}} + d_{\text{CS}} + d_{\text{BS}} + d_{\text{LS}} + d_{\text{JS}} \text{ (without long-term general scour)} \tag{28}$$

$$d_{\text{TS},2} = d_{L\text{-GS}} + d_{S\text{-GS}} + d_{\text{CS}} + d_{\text{BS}} + d_{\text{LS}} + d_{\text{JS}} \text{(including the long-term generalscour)} \tag{29}$$

Acknowledgments

The data provided by the Directorate General of Highways and the Water Resources Agency, Taiwan are gratefully acknowledged. The writers also wish to acknowledge Dr. Jun-Ji Lee for his valuable comments and technical assistance.

Notation

The following symbols are used in this paper:

b = pier width;
b_e = equivalent width of a pier;
b^* = caisson width;
d_{BS} = bend scour depth;
d_{CS} = contraction scour depth;
$d_{\text{CS},e}$ = equilibrium contraction scour depth;
d_{GS} = general scour depth attributed to flood induced (short-term general scour depth);
d_{JS} = Jet scour depth induced by the encased pipeline protection work;
d_{LS} = local scour depth below the surrounding bed level;
$d_{L\text{-GS}}$ = long-term general scour depth;
$d_{S\text{-GS}}$ = short-term general scour depth;
$d_{\text{TS},1}$ = total scour depth at the pier (without long-term general scour);
$d_{\text{TS},2}$ = total scour depth at the pier (including long-term general scour);
d_n = sediment size for which n% of the sediment is finer;
d_{50a} = median size of armor layer;
EL_B = bed elevation as bend scour occurred;
EL_c = caisson top level in the main channel;
EL_{ct} = caisson toe level;
EL_{fwl} = flood-level warning;
EL_L = bed elevation as local scour occurred;
EL_J = bed elevation as impinging jet scour occurred;
EL_p = top level of pipeline protection work;
EL_{SG} = bed elevation as short-term general scour occurred;
EL_{wf} = water stage as Pier 2 failed;
G_s = specific gravity;
K_{CS} = correction factor for contraction scour;
k_d = sediment size factor;
k_G = approach channel geometry factor;
k_I = flow intensity factor;
k_s = foundation shape factor;
k_t = time factor;
k_{yb} = flow depth-pier size factor;
k_θ = foundation alignment factor;
l = pier length;
L_c = caisson depth;
L_g = length of grade-control structure;
Q = flow discharge;
q = flow discharge per unit channel width;
r_c = center-line radius of bend curvature;
S_b = channel bed slope;
S_{rm} = downstream slope of protection work;
t = flood peak duration;
t_e = time for equilibrium scour;
V = average approaching flow velocity;

V_a = (for nonuniform sediments) mean velocity of flow at the "armor peak";
V_c = critical velocity for sediment entrainment;
V_{ca} = armoring critical velocity;
W = channel width;
W_1 = width of uncontracted section;
W_2 = width of contracted section;
x = distance;
Y = level of the top of the caisson measured from undisturbed sediment bed (positive downward);
y_{BS} = maximum scoured flow depth in a bend;
y_c = critical flow depth;
y_{ms} = flow depth from water surface to mean scoured (degraded) depth;
$y_{ms,c}$ = flow depth from water surface to mean scoured depth in a contracted section;
y_s = scoured flow depth;
y_u = average upstream un-scoured flow depth;
β = Contraction ratio, that is W_1/W_2;
θ = foundation alignment with respect to flow direction;
θ_{ca} = critical stress for armor layer; and
σ_g = Geometric standard deviation for particle size distribution, $\sigma_g = (d_{84}/d_{16})^{0.5}$.

References

Blench, T. (1969). *Mobile-bed fluviology*, Univ. of Alberta, Edmonton, Canada.

Bormann, N. E., and Julien, P. Y. (1991). "Scour downstream of grade-control structures." *J. Hydraul. Eng.*, 117(5), 579–594.

Chatley, H. (1931). "Curvature effects in open channels." *Engineering*, Vol. 131, London.

Dey, S., and Raikar, R. V. (2005). "Scour in long contractions." *J. Hydraul. Eng.*, 131(12), 1036–1049.

Lacey, G. (1930). "Stable channels in alluvium, Paper 4736." *Minutes of the Proc., Institution of Civil Engineers*, Vol. 229, William Clowes and Sons, London, 259–292.

Laursen, E. M. (1960). "Scour at bridge crossings." *J. Hydraul. Div.*, 86(2), 39–53.

Maza A., J. A., and Echavarria A., F. J. (1973). "Contribution to the study of general scour." *Proc., Int. Symp on River Mechanics*, IAHR., Bangkok, Thailand, 795–803.

Melville, B. W., and Coleman, S. E. (2000). *Bridge scour*, Water Resources Publication, Littleton, CO.

Neill, C. R. (1968). "Note on initial movement of coarse uniform bed material." *J. Hydraul. Res.*, 6(2), 173–176.

Raudkivi, A. J. (1990). *Loose boundary hydraulics*, 3rd Ed., Pergamon Press.

Richardson, E. V., and Davis, S. R. (1995). "Evaluating scour at bridges." *Hydr. Engrg. Circular No. 18: FHWA-IP-90-017*, Office of Engineering, Bridge Division, Washington, DC.

Thorne, C. R. (1988). "Bank processes on the Red River between Index, Arkansas, and Shreveport, Louisiana." *Final Rep. to the U.S. Army Eur. Res. Ofc., Contract No. DAJA45-88-C0018*, Dept. of Geography, Queen Mary College, London.

Water Resources Planning Institute. (2008). *Review Report on Dajia River Basin Integrated Regulation Plan*, Water Resources Agency, Taichung, Taiwan (in Chinese).